SBA-15 Templated Mesoporous Carbon: New Insights into the SBA-15 Pore Structure

Abdelhamid Sayari* and Yong Yang

Centre for Catalysis Research and Innovation (CCRI), Department of Chemistry, University of Ottawa, Ottawa, Ontario K1N 6N5, Canada

Received May 7, 2005. Revised Manuscript Received August 2, 2005

This work used a combination of designed synthesis conditions for SBA-15 to gain new insights into the genesis of micropores and secondary mesopores bridging the primary mesoporous channels. Different SBA-15 samples were prepared at low temperature (35 and 60 °C) without stirring to generate a simple monodispersed rodlike morphology. Sodium chloride was used to control the occurrence of micropores. All samples were used as templates for the synthesis of CMK-5 type (nanopipes) of porous carbons via carbonization of occluded poly(furfuryl alcohol). Detailed characterization of the silica templates, the carbon/silica composites, and the nanoporous carbons led to the following main conclusions: (i) Combination of inorganic salts with low synthesis temperature (ca. 35 °C) afforded SBA-15 silica free of micropores and secondary mesopores, akin to MCM-41. The corresponding carbon was fibrous in nature and did not retain the rodlike morphology of the template; (ii) the microporous as well as mesoporous bridges connecting the primary mesoporous channels of SBA-15 occur at temperatures as low as 60 °C. As the synthesis temperature increases, the microporous bridges tend to vanish, whereas the mesoporous bridges become more abundant. The corresponding carbon nanopipes, and by inference nanorods, exhibited the same morphology as the template.

Introduction

As described in many authoritative reviews,[1] much progress has been made in recent years in the synthesis and applications of ordered mesoporous materials (OMMs). Besides MCM-41, mesoporous SBA-15 silica is probably the most investigated OMM.[1−7] The following features contributed to the strong popularity of SBA-15 silica: (i) it can be easily and reproducibly prepared within a wide range of temperature (35−130 °C) using tetraethyl orthosilicate or cheaper sodium silicate;[3,8] (ii) it exhibits controllable pore sizes ranging from ca. 5 to 30 nm;[2−4] (iii) it has thick pore walls (2−6 nm), leading to improved thermal and hydrothermal stability; and (iv) it may exhibit a large variety of morphologies depending on the synthesis conditions.[3,9−12] With regard to its pore structure, it was initially thought of as an array of hexagonally packed cylindrical channels similar to MCM-41. However, it was soon realized that the SBA-15 pore structure is more complex. Detailed adsorption studies showed that, in addition to mesoporosity, SBA-15 silicas exhibit a significant amount of micropores. This was demonstrated using both the α_s-plot and the so-called geometrical model.[6] It was reported that the micropores in SBA-15 silica can be filled selectively by Pt deposition via γ-radiation treatment.[13] Moreover, the templating polymer within both mesopores and micropores can be removed stepwise.[14] Based on the successful synthesis of SBA-15 platinum[15,16] and carbon replicas,[17] it was inferred in early studies[6,17] that the micropores actually connect the mesoporous channels, thus allowing for the replica to be stable after the silica removal. Such direct transcription of the silica mesophase structure was not possible for the otherwise similar, but nonmicroporous, MCM-41 silica.[15,18]

* Corresponding author. E-mail: abdel.sayari@science.uottawa.ca.

(1) (a) Sayari, A. In *The Chemistry of Nanostructured Materials*; Yang, P., Ed.; World Scientific: River Edge, NJ, 2003; Chapter 2. (b) Sayari, A. In *Encyclopedia of Supramolecular Chemistry*; Atwood, J. L., Steed, J. W., Eds.; Marcel Dekker: New York, 2004; p 852. (c) Stein, A. *Adv. Mater.* **2003**, *15*, 763. (d) Sayari, A. *Chem. Mater.* **1996**, *8*, 1840. (e) Sayari, A.; Hamoudi, S. *Chem. Mater.* **2001**, *13*, 3151.
(2) Zhao, D. Y.; Feng, J. L.; Huo, Q. S.; Melosh, N.; Fredrickson, G. H.; Chemelka, B. F.; Stucky, G. D. *Science* **1998**, *279*, 548.
(3) Sayari, A.; Han, B.-H.; Yang, Y. *J. Am. Chem. Soc.* **2004**, *126*, 14348.
(4) Zhao, D. Y.; Huo, Q. S.; Feng, J. L.; Chmelka, B. F.; Stucky, G. D. *J. Am. Chem. Soc.* **1998**, *120*, 6024.
(5) Impéror-Clerc, M.; Davidson, P.; Davidson, A. *J. Am. Chem. Soc.* **2000**, *122*, 11925.
(6) Kruk, M.; Jaroniec, M.; Ko, C. H.; Ryoo, R. *Chem. Mater.* **2000**, *12*, 1961.
(7) Miyazawa, K.; Inagaki, S. *Chem. Commun.* **2000**, 2121.
(8) (a) Kim, S.-S.; Pauly, T. R.; Pinnavaia, T. J. *Chem. Commun.* **2000**, 1661. (b) Kim, J. M.; Stucky, G. D. *Chem. Commun.* **2000**, 1159.
(9) Fan, J.; Lei, J.; Wang, L.; Yu, C.; Tu, B.; Zhao, D. *Chem. Commun.* **2003**, 2140.
(10) Zhao, D.; Sun, J.; Li, Q.; Stucky, G. D. *Chem. Mater.* **2000**, *12*, 275.
(11) Zhao, D.; Yang, P.; Chmelka, B. F.; Stucky, G. D. *Chem. Mater.* **1999**, *11*, 1174.
(12) Yu, C.; Fan, J.; Tian, B.; Zhao, D.; Stucky, G. D. *Adv. Mater.* **2002**, *14*, 1742.
(13) Yamada, T.; Zhou, H.-S.; Hiroishi, D.; Tomita, M.; Ueno, Y.; Asai, K.; Honma, I. *Adv. Mater.* **2003**, *15*, 511.
(14) Lu, A.-H.; Schmidt, W.; Spliethoff, B.; Schüth, F. *Chem. Eur. J.* **2004**, *10*, 6085.
(15) Ryoo, R.; Ko, C. H.; Kurk, M.; Antochshuk, V.; Jaroniec, M. *J. Phys. Chem. B* **2000**, *104*, 11465.
(16) Galarneau, A.; Cambon, H.; Di Renzo, F.; Fajula, F. *Langmuir* **2001**, *17*, 8328.
(17) Jun, S.; Joo, S. H.; Ryoo, R.; Kruk, M.; Jaroniec, M.; Liu, Z.; Ohsuna, T.; Terasaki, O. *J. Am. Chem. Soc.* **2000**, *122*, 10712.
(18) Tian, B.; Che, S.; Liu, Z.; Liu, X.; Fan, W.; Tatsumi, T.; Terasaki, O.; Zhao, D. *Chem. Commun.* **2003**, 2726.

10.1021/cm050960q CCC: $30.25
Published on Web 10/26/2005

However, additional studies showed that when the synthesis temperature is above 80 °C, the connecting tunnels become mesoporous in nature.[16,19,20] When SBA-15 silicas prepared at above 80 °C are used as template, ordered mesoporous carbon rods (CMK-3)[15,17,21] and pipes (CMK-5)[22,23] with 2-D hexagonal symmetry were synthesized successfully. The carbon particles were stabilized by carbon bridges formed within micropores and/or secondary mesopores connecting the primary mesoporous channels of the SBA-15 templates. Similarly, SBA-15 was used as template to generate platinum replica, containing bridges between parallel rods, which were observed directly by TEM.[19] Notice that, in the great majority of studies, SBA-15 was prepared at 80−100 °C. This casts some doubt as to whether the micropores are actually bridging the main mesoporous channels as inferred in early studies[6,17] or not. Further work is needed to discriminate between bridging micropores, if any, and bridging mesopores.

It was also speculated that when the synthesis temperature is low, i.e., 30−40 °C, the pore walls of the material are too thick (ca. 4 nm) for the microporous channels to actually connect adjacent cylindrical mesopores.[19] In addition to the synthesis temperature, some other means to control the occurrence of micropores were reported. In particular, it was found that inorganic salts such as KCl, NaF, and NaCl have the ability to inhibit the formation of micropores during the synthesis of SBA-15.[3,12,24−26]

To date, SBA-15 templated mesoporous carbons (CMK-3 and CMK-5) were synthesized using SBA-15 silica samples with the conventional fibrous morphology.[2,9] The only exception was the CMK-3 type carbon prepared by Yu et al.[12] using monodispersed SBA-15 rods. Moreover, there are no reports about purely mesoporous SBA-15 without bridging tunnels. In this work, we used monodispersed rodlike SBA-15 samples with and without microporosity to synthesize various CMK-5 type carbons and to gain new insights into the genesis of SBA-15 pore structure versus temperature. In particular, answers to the following questions were sought: Is it possible to prepare a SBA-15 silica akin to MCM-41, i.e., purely mesoporous with no connecting bridges? Is it possible to discriminate between connecting micropores, if any, and connecting mesopores? Can such bridges occur selectively?

Experimental Section

Materials. Four SBA-15 silica samples with monodispersed rodlike morphology were synthesized at 35 or 60 °C in the presence or absence of sodium chloride using the method described earlier.[3] These samples will be denoted as **A**−**D**. Sample **A** was synthesized using the following gel composition 1:6:0.5:0.017:196 TEOS:HCl:NaCl:P123:H_2O. Typically, 4 g of P123 surfactant and 1.2 g of NaCl were dissolved in 120 g of 2 M HCl and 30 g of distilled water at 35 °C overnight under magnetic stirring. TEOS (8.5 g) was added while the solution was stirred. The stirring was maintained for 8 min at the same temperature and then stopped. This mixture was kept under static conditions at 35 °C for 48 h. The other samples **B**, **C**, and **D** were synthesized using the gel composition 1:6:*x*:0.017:196 TEOS:HCl:NaCl:P123:H_2O, where $x = 0$, 0.1, and 0.5. After TEOS was added and the mixture was stirred for 8 min, the mixture was kept under static conditions at 35 °C for 24 h and then at 60 °C for 24 h. All silica products were filtered, washed with distilled water, dried under ambient conditions, and calcined in air at 550 °C for 5 h. The calcined silica samples were aluminated using an aqueous solution $AlCl_3$ (Si/Al = 20) to generate catalytic sites for the polymerization of furfuryl alcohol. After evaporation of water at 80 °C overnight, the samples were calcined in air at 550 °C.

Mesoporous carbons were prepared using the above catalytically active SBA-15 as templates using the following procedure.[23] The pores of Al-modified silica templates were filled with furfuryl alcohol ($FA/SiO_2 = 1.5$ w/w) by incipient wetness at room temperature. The FA-filled SBA-15 materials were heated in an autoclave to 60 °C for 2 h and then to 150 °C for 5 h for polymerization. The polymer/SBA-15 samples were evacuated at 80 °C for 5 h before further carbonization. The carbonization was performed in a quartz cell under vacuum at 900 °C for 5 h. The resulting carbon/silica composites were denoted as **CP-A** to **CP-D** depending on the SBA-15 template used. Finally, the template silica walls were removed with 5% HF solution. The obtained nanoporous carbon samples were designated **NC-A** to **NC-D**.

Methods. X-ray diffraction patterns of all samples were recorded using a Scintag X_2 Advanced Diffraction System equipped with a solid-state detector using Cu Kα radiation with 0.15418 nm wavelength, a step size of 0.02° 2θ, and a counting time per step of 4.0 s over a $0.6° < 2\theta < 7°$ range. Scanning electron microscopy (SEM) images were collected on a JEOL-6400 instrument. Transmission electron micrographs (TEM) were obtained using a JEOL 2100F operated at 200 kV. Before examination, the specimen were dispersed in anhydrous ethanol and deposited on a holey carbon film on a copper grid. Nitrogen adsorption experiments were performed at 77 K using a Coulter Omnisorp 100 gas analyzer. Samples were evacuated at 200 °C for several hours to remove the surface humidity and pre-adsorbed gases before exposure to nitrogen. The specific surface area, S_{BET}, was determined from the linear part of the BET plot ($P/P_0 = 0.05-0.15$). The average pore size was the peak value on the pore size distribution (PSD), which was calculated from the adsorption branch using the KJS (Kruk, Jaroniec, Sayari) method.[27] The total pore volume, V_t, was determined from the amount of liquid N_2 adsorbed at a relative pressure of about 0.99. The micropore volume, V_m, was calculated using the α_s-plot method in the α_s range from 0.7 to 1.1. The α_s-values for SBA-15 sample were calculated by curve fitting of the standard α_s values for LiChrospher Si-1000 silica provided in the literature.[28]

Results

SBA-15 Silicas. XRD patterns of SBA-15 silicas are shown in Figure 1. Three peaks that can be indexed as (100),

(19) Galarneau, A.; Cambon, H.; Di Renzo, F.; Ryoo, R.; Choi, M.; Fajula, F. *New J. Chem.* **2003**, *27*, 73.
(20) Fan, J.; Yu, C.; Wang, L.; Tu, B.; Zhao, D.; Sakamoto, Y.; Terasaki, O. *J. Am. Chem. Soc.* **2001**, *123*, 12113.
(21) Ryoo, R.; Joo, S. H.; Kruk, M.; Jaroniec, M. *Adv. Mater.* **2001**, *13*, 677.
(22) Joo, S. H.; Choi, S. J.; Oh, I.; Kwak, J.; Liu, Z.; Terasaki, O.; Ryoo, R. *Nature* **2001**, *412*, 169.
(23) Kruk, M.; Jaroniec, M.; Kim, T.-W.; Ryoo, R. *Chem. Mater.* **2003**, *15*, 2815.
(24) Yu, C. Z.; Tian, B. Z.; Fan, J.; Stucky, G. D.; Zhao, D. Y. *Chem. Commun.* **2001**, 2726.
(25) Newalkar, B. L.; Choudary, N. V.; Turaga, U. T.; Vijayalakshmi, R. P.; Kumar, P.; Komarneni, S.; Bhat, T. S. G. *Chem. Mater.* **2003**, *15*, 1474.
(26) Newalkar, B. L.; Komarneni, S. *Chem. Mater.* **2001**, *13*, 4573.
(27) Kruk, M.; Jaroniec, M.; Sayari, A. *Langmuir* **1997**, *13*, 6267.
(28) Jaroniec, M.; Kruk, M.; Olivier, J. P. *Langmuir* **1999**, *15*, 5410.

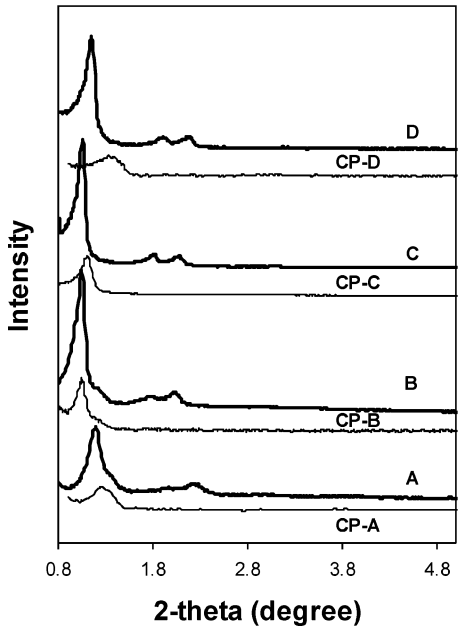

Figure 1. XRD patterns for SBA-15 silica templates and the corresponding SBA-15/carbon composites.

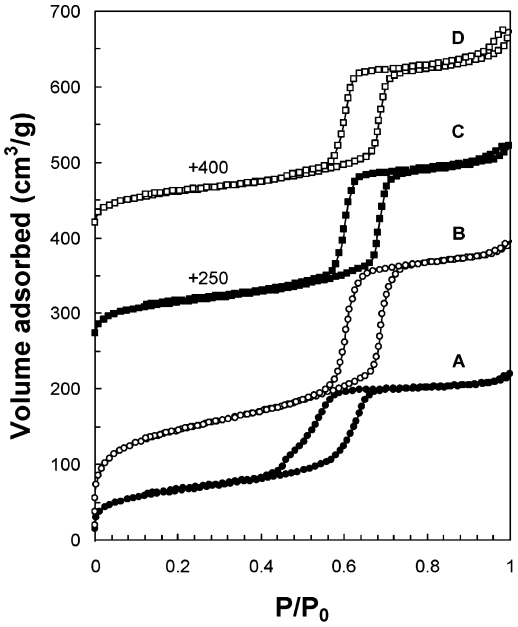

Figure 2. Nitrogen adsorption isotherms for SBA-15 templates. Isotherms for **C** and **D** were shifted upward by 250 and 400 units, respectively.

(110), and (200) diffractions are associated with *p*6*mm* hexagonal symmetry typical for SBA-15 materials. The corresponding nitrogen adsorption isotherms are shown in Figure 2. All samples exhibited an adsorption−desorption hysteresis loop indicative of the occurrence of pores larger than 4 nm.[29] Moreover, all samples exhibited narrow pore size distributions (Figure 3). The structural properties derived from adsorption data are listed in Table 1. Sample **A** made at 35 °C had the smallest pore size (6.5 nm) while the samples prepared at 60 °C exhibited similar pore sizes of ca. 7.5 nm. This is consistent with earlier findings regarding the effect of synthesis temperature on the pore size.[3] Sample **B** exhibited the highest surface area (530 m^2/g) and pore volume (0.61 cm^3/ g). The pore wall thickness *b* decreased with increasing amounts of added NaCl. Comparative α_s-plot (Figure 4) analysis of these SBA-15 samples indicated that only sample **B** had appreciable amounts of micropores (0.06 cm^3/g), whereas no indication of microporosity was observed in inorganic salt-added samples. This is consistent with earlier observations regarding the effect of inorganic salts on the occurrence of micropores.[3,12,24−26]

(29) Sayari, A.; Liu, P.; Kruk, M.; Jaroniec, M. *Chem. Mater.* **1997**, *9*, 2499

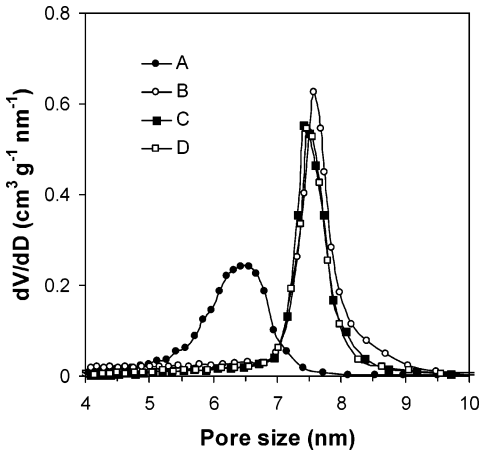

Figure 3. Pore size distribution for SBA-15 templates.

Table 1. Structural Properties of SBA-15, SBA-15/Carbon Composites, and Nanoporous Carbons[a]

sample[b]	*a* (nm)	S_{BET} ($m^2\,g^{-1}$)	V_t ($cm^3\,g^{-1}$)	w_{KJS} (nm)	*b* (nm)
A	8.7	238	0.34	6.5	2.2
B	9.7	530	0.61	7.6	2.1
C	9.4	235	0.41	7.4	2.0
D	8.7	224	0.27	7.5	1.2
CP-A	8.1	233	0.18	3.6	4.5
CP-B	9.7	327	0.18	3.6	5.1
CP-C	8.9	222	0.14	3.8	4.9
CP-D	7.7	256	0.15	3.8	3.9
NC-A	NA	558	0.56	NA	NA
NC-B	11.1	957	0.72	3.6	7.5
NC-C	9.4	1044	0.92	4.1	5.3
NC-D	9.7	1068	0.92	3.7	6.0

[a] *a*: unit-cell parameter; S_{BET}: BET specific surface area; V_t: total pore volume; w_{KJS}: pore diameter calculated using the KJS method;[27] *b*: pore wall thickness; NA: not available. [b] Sample **A** was prepared at 35 °C with $NaCl/SiO_2 = 0.5$; sample **B** was prepared at 60 °C with no salt; samples **C** and **D** were synthesized at 60 °C with $NaCl/SiO_2 = 0.1$ and 0.5, respectively.

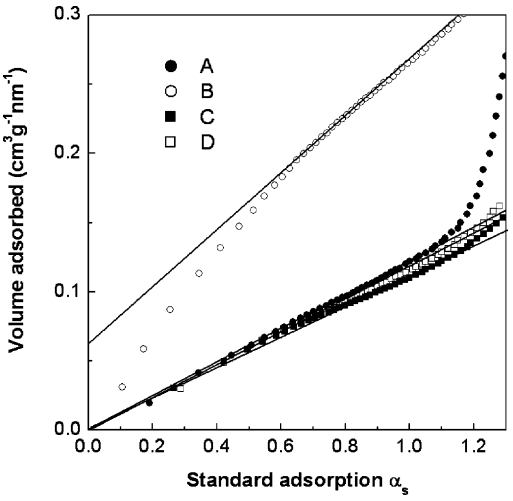

Figure 4. Comparative α_s-plots for SBA-15 templates.

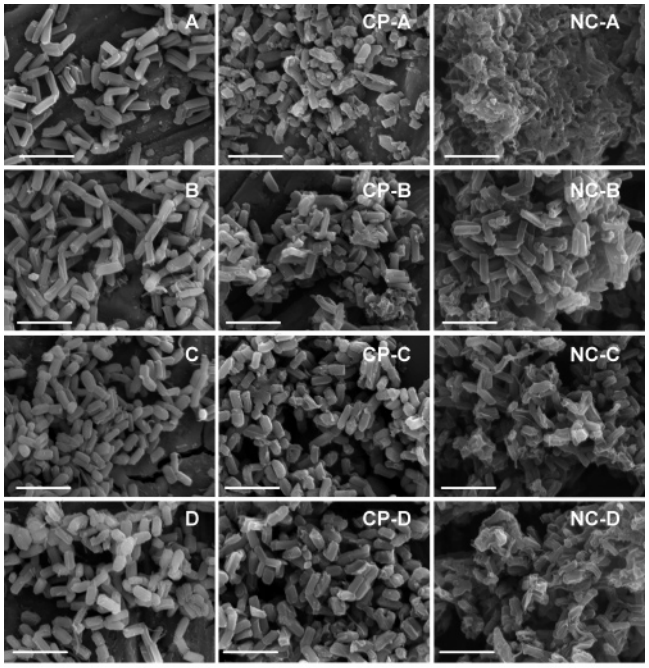

Figure 5. SEM images of SBA-15 template series (left), SBA-15/carbon composites (center), and mesoporous carbons (right). The bar length in all images = 3 μm.

SEM images of SBA-15 samples indicated that they have similar morphology, i.e., uniform rodlike particles with ca. 0.5 μm average diameter and 1−1.5 μm long (Figure 5, left images). It is known that this type of morphology can be obtained under static conditions using TEOS[3] or sodium silicate.[30] Samples with such a morphology have been investigated in detail elsewhere.[3]

SBA-15/Carbon Composites. XRD patterns of SBA-15/carbon composites (Figure 1) exhibited much lower overall intensity and decreased unit-cell size in comparison to the corresponding SBA-15 silica templates. This can be attributed to the occurrence of carbon lining the internal surface of the mesopore channels. Nitrogen adsorption data (Table 1) of these composites gave much lower adsorption volumes and surface areas in comparison to the corresponding silica templates. Nevertheless, the porosity was still present. The pore size for all composites was between 3.6 and 3.8 nm, suggesting that a layer of carbon with a thickness of ca.1.8 nm formed within the template channels. SEM images (Figure 5, **CP-A** to **CP-D**) of the composites indicated that the rodlike morphology of SBA-15 templates was preserved upon carbonization of the occluded polymer.

Mesoporous Carbons. All composites were treated with a 5% HF solution to remove the silica templates, thus leading to nanoporous carbons. TGA analysis of selected carbon samples indicated that all carbon burned out in air below 570 °C, and almost no silica residue (<0.3%) was left, indicating that the removal of silica was quantitative.

The XRD patterns of carbon samples are shown in Figure 6. For sample **NC-A**, no significant diffraction peaks were obtained, suggesting that this carbon sample had lost the original hexagonal mesostructure of the corresponding composites. This indicates that the ordered pore system was destroyed upon silica removal. In contrast, the XRD patterns of other carbon samples gave diffractions in a 2θ range close to that of the corresponding silica templates and silica/carbon composites. The relative intensity of the diffraction peaks changed. Consistent with literature data,[23] the main (100) peak decreased dramatically whereas other peaks, especially the (110) peak, increased significantly. The overall intensity decreased with increasing amounts of NaCl added during SBA-15 synthesis.

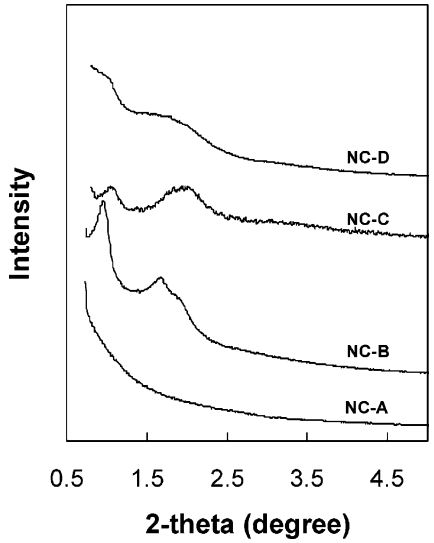

Figure 6. XRD patterns of ordered mesoporous carbons.

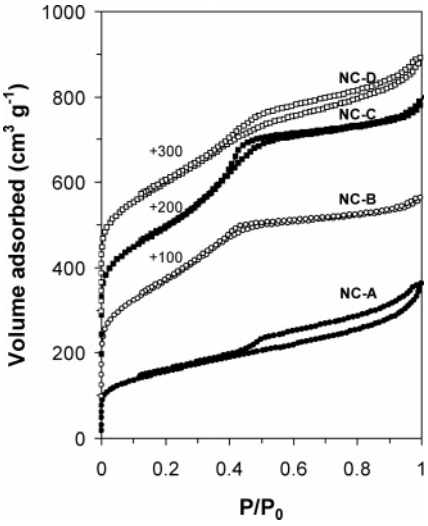

Figure 7. Nitrogen adsorption isotherms for nanoporous carbons. Isotherms were shifted upward by the amounts shown on the left-hand side.

The nitrogen adsorption isotherms (Figure 7) of carbon samples indicated that, except for **NC-A**, all other samples exhibited mesoporosity as evidenced by a relatively broad step on nitrogen adsorption isotherms and the corresponding pore size distributions (Figure 8).

SEM images (Figure 5, **NC-A** to **NC-D**) of these carbon materials show different morphologies. Sample **NC-B** retained the rodlike morphology of the parent composite, whereas samples **NC-C** and **NC-D** retained the same morphology, but to a lesser degree. As for sample **NC-A**, not a single rod was observed, but rather a web of nanotubes was obtained, indicating the collapse of the rodlike morphol-

(30) Kosuge, K.; Sato, T.; Kikukawa, N.; Takemori, M. *Chem. Mater.* **2004**, *16*, 899.

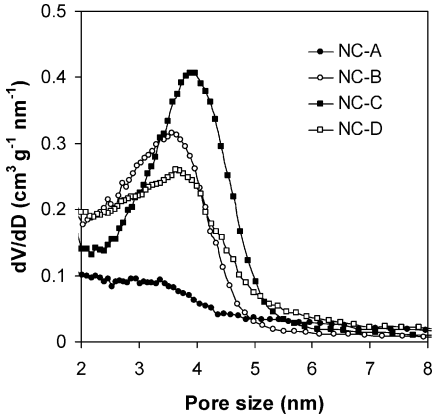

Figure 8. Pore size distributions for nanoporous carbons.

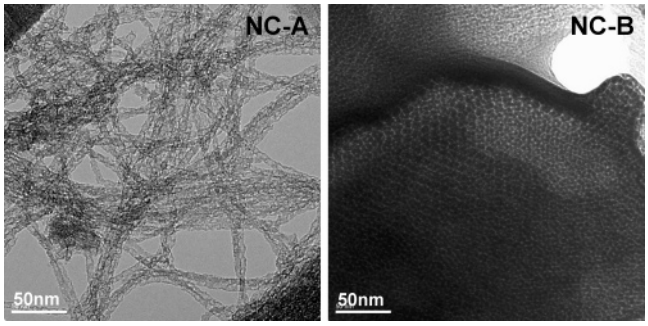

Figure 9. TEM images of fiberlike sample **NC-A** and rodlike sample **NC−B**.

ogy of the parent composite upon silica removal. This is consistent with the XRD and nitrogen adsorption data. Moreover, the TEM image for sample **NC-A** (Figure 9) shows that this material is comprised of randomly oriented fibers. On the contrary, the TEM image of sample **NC-B** viewed along the main axis shows a well-organized pore system with hexagonal symmetry (Figure 9)

Discussion

Based on literature data, SBA-15 silica made at 35 °C exhibits thick pore walls and micropores that are too short to connect adjacent mesoporous channels.[19] As the synthesis temperature increases to 80−100 °C, the pore walls become thinner and the mesoporous channels become connected by bridges regarded by some authors as microporous in nature[6,15,17] and by others as mesoporous.[16,19] At even higher temperature, i.e., 130 °C, the micropores tend to vanish, whereas the secondary mesopores bridging the main channels still occur.[19,20]

To shed further light into the genesis of bridging micropores if any, and bridging mesopores, the current work used a combination of three tools: (i) low synthesis temperature (35 and 60 °C), (ii) use of NaCl to control the occurrence of micropores, and (iii) synthesis of SBA-15 templated carbon to check the occurrence of interconnecting bridges. All SBA-15 samples were prepared without stirring to obtain a simple rodlike morphology.[3]

Despite the rodlike morphology of its silica precursor **A**, the **NC-A** carbon sample did not exhibit a single rodlike particle. XRD and nitrogen adsorption data showed that this sample lacked the hexagonal symmetry of its parent **CP-A**

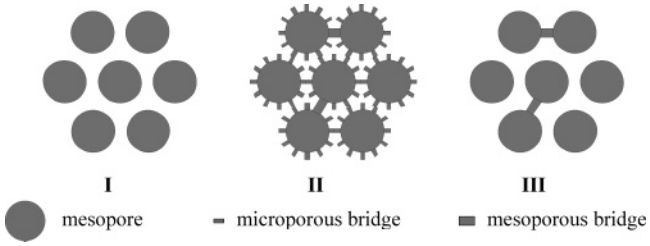

Figure 10. Schematic representation of SBA-15 silica templates prepared under different conditions. (I) Sample **A**, (II) sample **B**, and (III) samples **C** and **D**.

carbon/silica composite and had no particular order. The pore structure of the corresponding SBA-15 template can be illustrated as **I** in Figure 10, which consists of hexagonally packed mesoporous channels with no additional micropores and no interconnecting bridges. This structure prepared at low temperature (35 °C) in the presence of NaCl is reminiscent of MCM-41. Used as template, it affords carbon nanorods or nanopipes that are not connected together, the current **NC-A** material being an example.

Nitrogen adsorption data and the α_s-plot indicated the presence of microporosity only in sample **B**, which was prepared at 60 °C in the absence of NaCl. The corresponding carbon **NC-B** retained completely the rodlike morphology, indicating that the template contained bridges interconnecting the main channels. However, though the occurrence of micropores is confirmed by the α_s-plot, the nature of the bridges remains at this stage unknown. It could be microprous, mesoporous, or both. As shown hereafter, based on the behavior of samples **B** and **C** and their corresponding carbons, it is inferred that, at 60 °C, both microporous and mesoporous bridges occur. Sample **C** was prepared in the presence of a small amount of NaCl ($NaCl/SiO_2 = 0.1$), which inhibited the formation of micropores, but did not affect the pore wall thickness (Table 1). The fact that the rodlike morphology of **CP-C** was partially preserved upon removal of silica (Figure 5, **NC-C**) indicates that the template **C**, and by inference **B**, had mesoporous bridges. However, as indicated by high-magnification SEM images (not shown), the rodlike morphology was better preserved in **NC-B** than in **NC-C**, providing strong evidence that the silica template **B** had additional microporous bridges. This indicates that secondary bridging mesopores form at a temperature as low as 60 °C, and there may not be a temperature range where only interconnecting micropores occur. Figure 10 **II** and **III** provide a schematic representation of the pore structure of materials **B** and **C**, respectively. Sample **D** is basically similar to sample **C**, except that it has thinner walls, most likely because of the increased amount of salt used in the synthesis mixture.

Based on the fact that the morphology of **CP-C** and **CP-D** was partially stable upon removal of silica, it was inferred that, in the absence of micropores, SBA-15 samples prepared at 60 °C, i.e., **C** and **D**, contained a limited number of mesoporous bridges. To verify the role of connecting mesopores, an additional CMK-5 type nanoporous carbon was prepared using a SBA-15 template synthesized at higher temperature (80 °C) in the presence of NaCl ($NaCl/SiO_2 = 0.5$). Nitrogen adsorption data and α_s-plot analysis indicated

that this SBA-15 was micropore-free. The corresponding carbon retained the rodlike morphology perfectly, suggesting that, at higher synthesis temperature, more secondary mesoporous bridges occur within the SBA-15 template, leading to carbon nanopipes particles with enhanced stability.

Conclusion

By combining the effect of inorganic salts with low synthesis temperature (ca. 35 °C), it was possible to synthesize SBA-15 silica with monodispersed rodlike morphology free of micropores and secondary mesopores, like MCM-41. Using this material as template afforded fibrous carbon.

Microporous as well as mesoporous bridges connecting the primary mesoporous channels of SBA-15 occur at temperatures as low as 60 °C. As the synthesis temperature increases, the microporous bridges tend to vanish, whereas the mesoporous bridges become more abundant. The corresponding carbon nanopipes, and by inference nanorods, exhibit the same morphology as the template.

Acknowledgment. The financial support of the Natural Sciences and Engineering Council of Canada is acknowledged. A.S. thanks the Canadian Government for a Canada Research Chair in Catalysis by Nanostructured Materials (2001−2008).

CM050960Q